Synthesis and properties of 5-aza-15-thiaporphyrins

Daisuke Yamashita, Hiroto Omori, Norihito Fukui and Hiroshi Shinokubo*

Department of Molecular and Macromolecular Chemistry, Graduate School of Engineering, Nagoya University, Chikusa-ku, Nagoya 464-8603, Japan

Dedicated to Professor Atsuhiro Osuka on the occasion of his 65th birthday

Received date (to be automatically inserted after your manuscript is submitted)
Accepted date (to be automatically inserted after your manuscript is accepted)

ABSTRACT: We have successfully prepared 5-aza-15-thiaporphyrin through nucleophilic sulfination of nitrogen-bridged dibromobisdipyrrin with sodium sulfide. X-ray diffraction analysis elucidated its structure in the solid state: two dipyrrin subunits were roughly coplanar around the sp^2-hybridized *meso*-nitrogen. In contrast, they adopted a folded conformation around the *meso*-sulfur atom. Due to its relatively distorted structure, 5-aza-15-thiaporphyrin shows weak antiaromaticity in the magnetic criteria. The sulfur atom was oxidized with *m*-chloroperbenzoic acid to provide 5-aza-15-thiaporphyrin *S*-dioxide in good yield. While 5-aza-15-thiaporphyrin was non-emissive, its *S*-dioxide exhibited fluorescence in solution.

KEYWORDS: 5-aza-15-thiaporphyrin, antiaromaticity, heteroporphyrinoids, sulfide, sulfone

*Correspondence to: Hiroshi Shinokubo, e-mail: hshino@chembio.nagoya-u.ac.jp

INTRODUCTION

Recently, the synthesis, structures, and properties of porphyrinoids containing various heteroatoms at the *meso*-position have been extensively explored owing to the development of efficient synthetic procedures to access these interesting class of π-conjugated macrocyclic molecules [1]. In particular, the aromaticity/antiaromaticity of 5,15-diheteroporphyrins such as 18π diazaporphyrin **1** [2], 20π diazaporphyrin **2** [3], 20π dioxaporphyrin **3** [4], and 20π dithiaporphyrin **4** [5] have been disclosed (Fig 1). Among 20π diheteroporphyrins, 20π diazaporphyrin **2** and 20π dioxaporphyrins **3** are antiaromatic because of their planar conformation and 20π electrons along the π-conjugation circuit, while 20π dithiaporphyrin **4** is regarded as a non-aromatic porphyrin in the magnetic criteria. The lack of the paratropic ring current effect in 20π dithiaporphyrin **4** is originated from its folded structure around the *meso*-sulfur atoms.

In addition, 5,15-diheteroporphyrins with two different heteroatoms have been synthesized. Matano and co-worker have prepared a Zn(II) complex of 5-aza-15-oxaporphyrin **5** and its one- and two-oxidation species to examine their aromatic/antiaromatic character [6]. We then became interested in inclusion of both sulfur and nitrogen atoms to obtain 5-aza-15-thiaporphyrin **6**. We expected that the longer C–S bonds would substantially change the planar conformation of 20π diazaporphyrin **2**. Furthermore, oxidation of the sulfide linkage to the corresponding sulfone should result in significant change in their optoelectronic properties. Here we describe the synthesis and properties of 5-aza-15-thiaporphyrin **6** and its *S*-dioxide **7**.

((Fig 1))

RESULTS AND DISCUSSION

Treatment of nitrogen-linked dibromodipyrrin **8** [7] with sodium sulfide (1.0 equiv) in DMF at 65 °C for 10 h afforded 10,20-mesityl-5-aza-15-thiaporphyrin free-base **6** in 40% yield (Scheme 1). The formation of **6** was confirmed by the ^{1}H NMR spectroscopy and high-resolution mass spectrometry. The *β*-pyrrole protons of **6** appeared as four sets of doublet peaks at δ = 5.55, 5.77, 5.92, and 5.97 ppm (Fig 2). These signals are substantially upfield-shifted in comparison to the *β*-pyrrole protons of 5,15-dithiaporphyrin **4**, which were observed around δ = 6.3 ppm [5a]. Furthermore, these signals are also upfield-shifted rather than those of the precursor **8** (δ = 6.5–5.9 ppm). This shift is explained by the presence of the paratropic ring current effect in 5-aza-15-thiaporphyrin **6**, indicating its weak but non-negligible antiaromatic character (*vide infra*). However, the paratropic ring current effect of **6** is attenuated in comparison to that in 20π diazaporphyrins **2**, in which *β*-pyrrole protons appear around δ = 3.5–4.6 ppm [3]. The antiaromaticity of **6** is also reflected in its absorption property: The UV/vis absorption spectrum of **6** exhibits weak and broad absorption bands from 500 to 800 nm, which is a diagnostic feature of antiaromatic porphyrinoids (Fig 3a) [8]. The parent mass ion peak of **6** was observed at *m/z* = 687.3015 (calcd for $(C_{44}H_{41}N_5O_3S)^+$ = 687.3026 [(M^+)] in its high-resolution atmospheric-pressure-chemical-ionization time-of-flight (HR APCI-TOF) mass spectrum.

((Scheme 1))

((Fig 2))

((Fig 3))

The solid-state structure of **6** was unambiguously elucidated by X-ray diffraction analysis (Fig 4). Slow vapor diffusion of methanol into a chloroform solution of **6** afforded suitable crystals for X-ray diffraction analysis. The tetrapyrrolic macrocycle folds at the *meso*-sulfur atom with a dihedral angle of 151°. In contrast, two dipyrrin subunits are roughly coplanar around the sp^2-hybridized *meso*-nitrogen.

((Fig 4))

The antiaromaticity of **6** was further confirmed by the density functional theory (DFT) calculations. The ring current effect of **6** was evaluated by the nucleus-independent chemical shift (NICS) [9] and the anisotropy of the induced current density (ACID) [10] calculations. The positive NICS values (δ = 10–15) at the inner positions well supports the appreciable antiaromaticity of **6** (Fig 5a). Furthermore, the counter-clockwise current stream visualized by the ACID calculation also supports the paratropic ring current effect in **6** (Fig 5b).

((Fig 5))

To alter the optoelectronic property of sulfur-containing π-systems, oxidation of a sulfide moiety to the corresponding sulfoxide is effective. Consequently, the sulfur atom at the *meso*-position was oxidized. Treatment of 5-aza-15-thiaporphyrin free-base **6** with *m*-chloroperbenzoic acid (6.0 equiv) furnished the corresponding sulfone **7** in 65% yield (Scheme 2). The *β*-pyrrole protons of **7** were observed at δ = 6.87, 6.92, 7.18, and 7.42 ppm, indicating the loss of the paratropic ring current effect. The disappearance of the antiaromaticity of **6** could be attributed to the interruption of the macrocyclic π-conjugation due to the loss of the lone pair on sulfur. The UV/vis absorption spectrum of **7** displayed a feature of dipyrrin dimers (Fig 3a). While 5-aza-15-thiaporphyrin free-base **6** does not show any emission, fluorescence was detected in the case of its *S*-dioxide **7** (Fig 3b). This is probably associated with the loss of the antiaromaticity of **6**. The fluorescence quantum yield of **7** decreased as the solvent polarity increased. The quantum yields are 0.08 (cyclohexane), 0.08 (toluene), 0.06 (hexane), 0.03 (dichloromethane), 0.02 (acetone) and 0.03 (DMSO).

((Scheme 2))

EXPERIMENTAL

General

^{1}H NMR (500 MHz) and ^{13}C NMR (126 MHz) spectra were recorded on a Bruker AVANCE III HD spectrometer, and chemical shifts were reported as the delta scale in ppm relative to $CHCl_3$ (δ = 7.260 ppm) for ^{1}H NMR and $CDCl_3$ (δ = 77.16 ppm) for ^{13}C NMR. UV/vis/NIR absorption spectra were recorded on a Shimadzu UV-2550 or JASCO V670 spectrometer. High-resolution mass spectra were recorded on a Bruker microTOF-II using positive mode APCI-TOF method for acetonitrile solutions. X-ray crystallographic data of **6** was taken on a Rigaku CCD diffractometer (Saturn 724 with MicroMax-007) with Varimax Mo optics using graphite monochromated Mo-Kα radiation (λ = 0.71075 Å). Dry toluene was prepared by distillation from CaH_2 and degassed by N_2 bubbling. Unless otherwise noted, materials obtained from commercial suppliers were used without further purification.

Synthesis

Preparation of *N*,*N*-bis(1-bromo-5-mesityl-dipyrrin-9-yl)-*N*-(4-methoxybenzyl)amine 8. A Schlenk tube containing 1,9-dibromo-5-mesityldipyrrin (418 mg, 0.995 mmol), $Pd_2(dba)_3 \cdot CHCl_3$ (25.9 mg, 25.0 μmol), Xantphos (28.8 mg, 49.8 μmol), KO*t*Bu (282 mg, 2.51 mmol) was evacuated and the refilled with argon. To the tube, 4-methoxybenzylamine (104 μL, 0.804 mmol) and dry toluene (15 mL) were added. The mixture was stirred at 80 °C for 30 min. The mixture was cooled to room temperature. The mixture was passed through short celite column eluting with CH_2Cl_2. The solvent was removed *in vacuo*. The residue was purified by silica gel column chromatography eluting with CH_2Cl_2/hexane. Recrystallization from CH_2Cl_2/MeOH afforded **8** (137 mg, 0.167 mmol, 34%). **8**. ^{1}H NMR ($CDCl_3$): δ, ppm 2.13 (s, 12H, Mes), 2.35 (s, 6H, Mes), 3.80 (s, 3H, 4-methoxybenzyl), 5.31 (s, 2H, 4-methoxybenzyl), 5.96 (d, J = 4.0 Hz, 2H, *β*), 6.15 (d, J = 4.0 Hz, 2H, *β*), 6.53–6.57 (m, 4H, *β*), 6.91–6.94 (m, 6H, Mes + 4-methoxybenzyl), 7.41 (d, J = 8.5 Hz, 2H, 4-methoxybenzyl), 12.62 (s, 2H, NH). ^{13}C NMR ($CDCl_3$): δ, ppm 20.16, 21.26, 53.20, 55.43, 114.11, 114.49, 115.36, 115.82, 121.04, 127.94, 129.60, 132.85, 133.23, 133.93, 136.17, 137.51, 142.73, 159.11, 160.27 (Some signals due to sp^2 carbons were too broad to be detected probably because the time scale of the tautomerization of inner NH protons is comparable to the NMR time scale). HR-MS (APCI-MS): *m/z* 813.1678 (calcd. for $[M]^+$ 813.1672).

Preparation of 10,20-dimesityl-5-aza-15-thiaporphyrin 6. To a solution of nitrogen-linked dibromodipyrrin dimer **8** (23.7 mg, 29.1 μmol) in DMF (8 mL) was added $Na_2S \cdot 9H_2O$ (7.01 mg, 29.1 μmol) portionwise. The mixture was stirred at 65 °C for 15 h. The mixture was extracted with AcOEt. The organic layer was washed with water, dried over Na_2SO_4, and then evaporated. The residue was purified by silica-gel column chromatography (EtOAc/hexane) to afford free-base 5-aza-15-thiaporphyrin **6** (8.00 mg, 11.6 μmol) in 40% yield as a green solid. **6**. ^{1}H NMR ($CDCl_3$): δ, ppm 2.16 (s, 12H, Mes), 2.29 (s, 6H, Mes), 3.78 (s, 3H, 4-methoxybenzyl), 4.68 (s, 2H, 4-methoxybenzyl), 5.55 (d, J = 4.5 Hz, 2H, *β*), 5.77 (d, J = 4.0 Hz, 2H, *β*), 5.92 (d, J = 4.6 Hz, 2H, *β*), 5.97 (d, J = 4.0 Hz, 2H, *β*), 6.83 (s, 4H, Mes), 6.88 (d, J = 6.5 Hz, 2H, 4-methoxybenzyl), 7.18 (d, J = 6.5 Hz, 2H, 4-methoxybenzyl), 14.87 (s, 2H, NH). ^{13}C NMR ($CDCl_3$): δ, ppm 19.92, 21.19, 53.62, 55.44, 114.57, 117.57, 127.35, 127.61, 127.79, 127.86, 129.24, 131.20, 134.26, 137.12, 137.22, 137.78, 142.45, 156.83, 159.21 (Some signals due to sp^2 carbons were too broad to be detected probably because the time scale of the tautomerization of inner NH protons is comparable to the NMR time scale). λ_{max}, nm (ε $M^{-1}.cm^{-1}$) 293 (2.5×10^4), 421 (8.1×10^4). HR-MS (APCI-MS): *m/z* 687.3015 (calcd. for $[M]^+$ 687.3026). Crystal data: $C_{44}H_{41}N_5OS$, M = 687.88, orthorhombic, space group P_{bca}, a = 18.2843(7), b = 15.3593(5), c = 26.5865(12) Å, V = 7466.4(5) Å^3, T = 93(2) K, Z = 8, D_c = 1.224 g.cm^{-3}, R = 0.0809 ($I > 2.0\ \sigma(I)$), R_w = 0.2316 (all data), GOF = 1.049 ($I > 2.0\ \sigma(I)$).

Preparation of 10,20-dimesityl-5-aza-15-thiaporphyrin *S*-dioxide 7. To a solution of **6** (14.9 mg, 21.7 μmol) in CH_2Cl_2 (10 mL) was added *m*-chloroperbenzoic acid (70%, 35.2 mg, 143 μmol). The mixture was stirring at room temperature for 5 min. The mixture was evaporated *in vacuo*. The mixture was purified by silica gel column chromatography (EtOAc/hexane) to afford 5-aza-15-thiaporphyrin *S*-dioxide **7** (10.2 mg, 14.1 μmol) in 65% yield as a red solid. **7**: ^{1}H NMR ($CDCl_3$): δ, ppm 2.00 (s, 12H, Mes), 2.41 (s, 6H, Mes), 3.78 (s, 3H, 4-methoxybenzy), 5.78 (s, 2H, 4-methoxybenzy), 6.87 (d, J = 5.0 Hz, 2H, *β*), 6.90 (d, J = 8.5 Hz, 2H, 4-methoxybenzy), 6.92 (d, J = 5.0 Hz, 2H, *β*), 6.99 (s, 4H, Mes), 7.18 (d, J = 5.0 Hz, 2H, *β*), 7.22 (d, J = 8.5 Hz, 2H, 4-methoxybenzy), 7.42 (d, J = 4.1 Hz, 2H, *β*), 8.29 (s, 2H, NH). ^{13}C NMR ($CDCl_3$): δ, ppm 20.61, 21.33, 55.40, 55.48, 114.30, 114.83, 117.20, 125.33, 127.05, 128.07, 128.40, 134.21, 134.38, 137.74, 137.89, 138.28, 138.73, 140.22, 141.18, 154.08, 159.67. λ_{max}, nm (ε $M^{-1}.cm^{-1}$) 409 (9.4×10^4), 456 (2.3×10^4). HR-MS (APCI-MS): *m/z* 720.3040 (calcd. for $[M + H]^+$ 720.3003).

DFT calculations

All calculations were performed using the Gaussian 09 program [11]. Geometries of **6** was obtained from its X-ray structure but the 4-methoxybenzyl group was replaced with a methyl group. The structure was fully optimized without any symmetry restriction at the Becke's three-parameter hybrid exchange functional and the Lee–Yang–Parr correlation functional (B3LYP) [12] with the def2-TZVP basis sets [13]. The NICS calculation was performed using gauge-including atomic orbitals (GIAOs) at the B3LYP/def2-TZVP level on the optimized geometry. The ACID calculation was performed at the CGST-B3LYP/def2-TZVP level on the optimized structure.

CONCLUSION

We have achieved the facile synthesis of 10,20-diaryl-5-aza-15-thiaporphyrin and its *S*-dioxide from a nitrogen-linked dibromodipyrrin precursor. The structure of 5-aza-15-thiaporphyrin was evaluated by means of X-ray diffraction analysis. The antiaromatic nature of 5-aza-15-thiaporphyrin was confirmed by ^{1}H NMR analysis and DFT calculations. Oxidation of the sulfur linkage to the sulfone moiety significantly changed the electronic property, resulting in the loss of the paratropic ring current effect and generation of fluorescence.

Acknowledgements

This work was supported by JSPS KAKENHI grants JP26102003 (HS) and JP17H01190 (HS). NF gratefully acknowledges the Tatematsu Foundation for financial support.

Supporting information

The CIF file for the crystal structure was deposited at the Cambridge Crystallographic Data Centre (CCDC). The CCDC deposition numbers of compound **6** is 1911373. These data can be obtained free of charge from the Cambridge Crystallographic Data Centre via www.ccdc.cam.ac.uk/data_request/cif.

REFERENCES

1. Matano Y. *Chem. Rev*. 2017; **117**: 3138-3191.
2. (a) Fischer H, Haberland H and Müller A. *Liebigs Ann. Chem*. 1936; **521**: 122-128. (b) Semeikin AS, Mamardashvili NZ, Glazunov AV, Golubchikov OA and Berezin BD. *Izv. Vyssh. Uchebn. Zaved., Khim. Khim. Tekhnol*. 1990; **33**: 12-16. (c) Khelevina OG, Chizhova NV, Stuzhin PA, Semeikin A and Berezin BD. *Russ. J. Phys. Chem*. 1997; **71**: 74-78. (d) Matano Y, Shibano T, Nakano H and Imahori H. *Chem. Eur. J*. 2012; **18**: 6208-6216. (d) Matano Y, Shibano T, Nakano H, Kimura Y and Imahori H. *Inorg. Chem*. 2012; **51**: 12879-12890. e) Horie M, Hayashi Y, Yamaguchi S and Shinokubo, H. *Chem. Eur. J*. 2012; **18**: 5919-5923.
3. (a) Sudoh K, Satoh T, Amaya T, Furukawa K, Minoura M, Nakano H and Matano Y. *Chem. Eur. J*. 2017; **23**: 16364-16373. (b) Satoh T, Minoura M, Nakano H, Furukawa K and Matano Y. *Angew. Chem. Int. Ed*. 2016; **55**: 2235-2238. (c) Yamaji A, Tsurugi H, Miyake Y, Mahima K and Shinokubo H. *Chem. Eur. J*. 2016; **22**: 3956-3961.
4. Nishiyama A, Fukuda M, Mori S, Furukawa K, Fliegl H, Furuta H and Shimizu S, *Angew. Chem. Int. Ed*. 2018; **57**: 9728-9733.
5. (a) Kamiya H, Kondo T, Sakida T, Yamaguchi S and Shinokubo H. *Chem. Eur. J*. 2012; **18**: 16129-16135. (b) Wachi N, Kondo T, Ito S, Hiroto S, Shin JY and Shinokubo H. *J. Porphyrins Phthalocyanines* 2014; **18**: 675-678. (c) Broadhurst MJ, Grigg R and Johnson AW. *J. Chem. Soc. Chem. Commun*. 1970; 807-809; (c) Broadhurst MJ, Grigg R and Johnson AW. *J. Chem. Soc. Perkin Trans. 1* 1972; 1124-1135.
6. Sudoh K, Furukawa K, Nakano H, Shimizu S and Matano Y. *Heteroatom Chem*. 2018; **29**: e21456.

7. (a) Omori H, Hiroto S and Shinokubo H. *Chem. Comm*. 2016; **52**: 3540-3543. (b) Omori H, Hiroto S and Shinokubo H. *Org. Lett*. 2016; **18**: 2978-2981.
8. Oh J, Sung YM, Hong Y and Kim D. *Acc. Chem. Res*. 2018; **51**: 1349-1358.
9. Chen Z, Wannere CS, Corminboeuf C, Puchta R and Schleyer PVR. *Chem. Rev*. 2005; **105**: 3842-3888.
10. Geuenich D, Hess K, Köhler F and Herges R. *Chem. Rev*. 2005; **105**: 3758-3772.
11. Frisch MJ, Trucks GW, Schlegel HB, Scuseria GE, Robb MA, Cheeseman JR, Scalmani G, Barone V, Mennucci B, Petersson GA, Nakatsuji H, Caricato M, Li X, Hratchian HP, Izmaylov AF, Bloino J, Zheng G, Sonnenberg JL, Hada M, Ehara M, Toyota K, Fukuda R, Hasegawa J, Ishida M, Nakajima T, Honda Y, Kitao O, Nakai H, Vreven T, Montgomery Jr., JA, Peralta JE, Ogliaro F, Bearpark M, Heyd JJ, Brothers E, Kudin KN, Staroverov VN, Kobayash, R, Normand J, Raghavachari K, Rendell A, Burant JC, Iyengar SS, Tomasi J, Cossi M, Rega N, Millam JM, Klene M, Knox JE, Cross JB, Bakken V, Adamo C, Jaramillo J, Gomperts R, Stratmann RE, Yazyev O, Austin AJ, Cammi R, Pomelli C, Ochterski JW, Martin RL, Morokuma K, Zakrzewski VG, Voth GA, Salvador P, Dannenberg JJ, Dapprich S, Daniels AD, Farkas Ö, Foresman JB, Ortiz JV, Cioslowski J and Fox DJ. *Gaussian 09, Revision D.01,* Gaussian Inc: Wallingford CT, 2009.
12. (a) Becke AD. *Phys. Rev. A* 1988; **38**: 3098-3100. (b) Lee C, Yang W, Parr RG. *Phys. Rev. B* 1988; **37**: 785-789.
13. (a) Schäfer A, Horn H and Ahlrichs R. *J. Chem. Phys.* 1992; **97**: 2571-2577. (b) Weigend F and Ahlrichs R. *Phys. Chem. Chem. Phys.* 2005; **7**: 3297-3305. (c) Eichkorn K, Weigend F, Treutler O and Ahlrichs R. *Theor. Chem. Acc.* 1997; **97**: 119-124.

Figures and Schemes Captions

Scheme 1. Preparation of 5-aza-15-thiaporphyrin free-base **6**.

Scheme 2. Preparation of 5-aza-15-thiaporphyrin *S*-dioxide **7**.

Fig 1. Examples of 5,15-diheteroporphyrins.

Fig 2. ^{1}H NMR spectra of (a) 5-aza-15-thiaporphyrin **6** and (b) 5,15-dithiaporphyrin **4** in $CDCl_3$.

Fig 3. (a) UV/vis absorption spectra of **6** and **7** measured in dichloromethane. (b) Fluorescence spectra of **7** in various solvents.

Fig 4. (a) Top and (b) side views of X-ray crystal structure of **6**. Mesityl and 4-methoxybenzyl groups as well as hydrogen atoms are omitted for clarity. Thermal ellipsoids are at the 50% probability level.

Fig 5. (a) NICS values of **6** calculated at the GIAO-B3LYP/def2-TZVP level. (b) ACID plot of **6** (isovalue 0.03) calculated at the CSGT-B3LYP/def2-TZVP level.

Scheme 1. Preparation of 5-aza-15-thiaporphyrin free-base **6**.

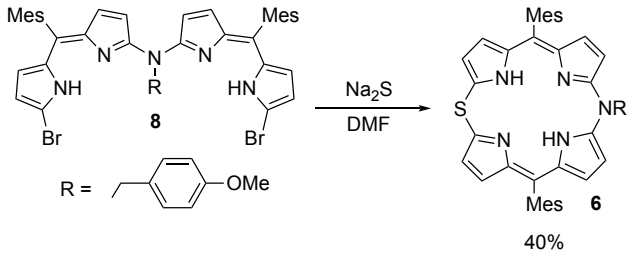

Scheme 2. Preparation of 5-aza-15-thiaporphyrin *S*-dioxide **7**.

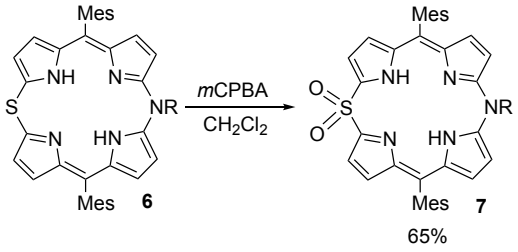

Fig 1. Examples of 5,15-diheteroporphyrins.

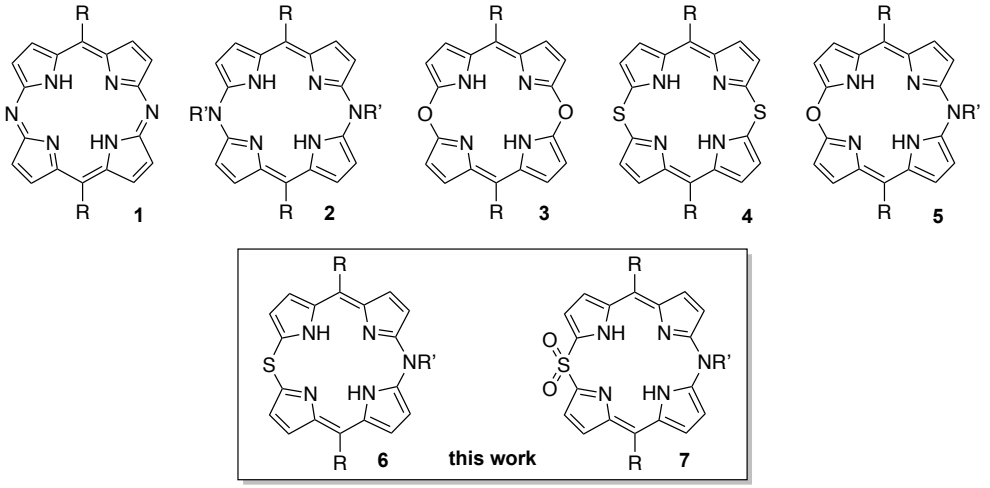

Fig 2. ^{1}H NMR spectra of (a) 5-aza-15-thiaporphyrin **6** and (b) 5,15-dithiaporphyrin **4** in $CDCl_3$.

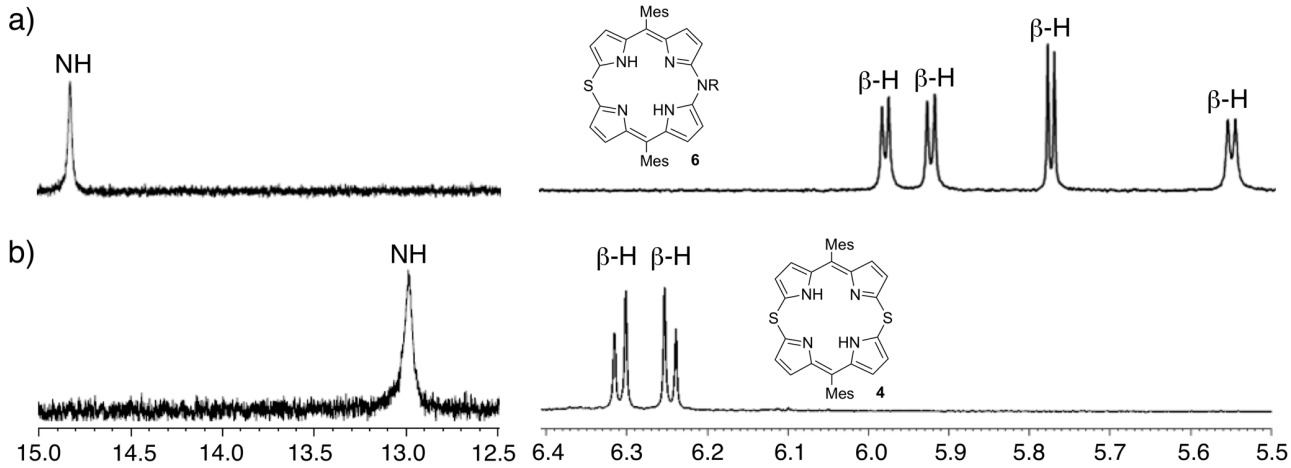

Fig 3. (a) UV/vis absorption spectra of **6** and **7** measured in dichloromethane. (b) Fluorescence spectra of **7** in various solvents.

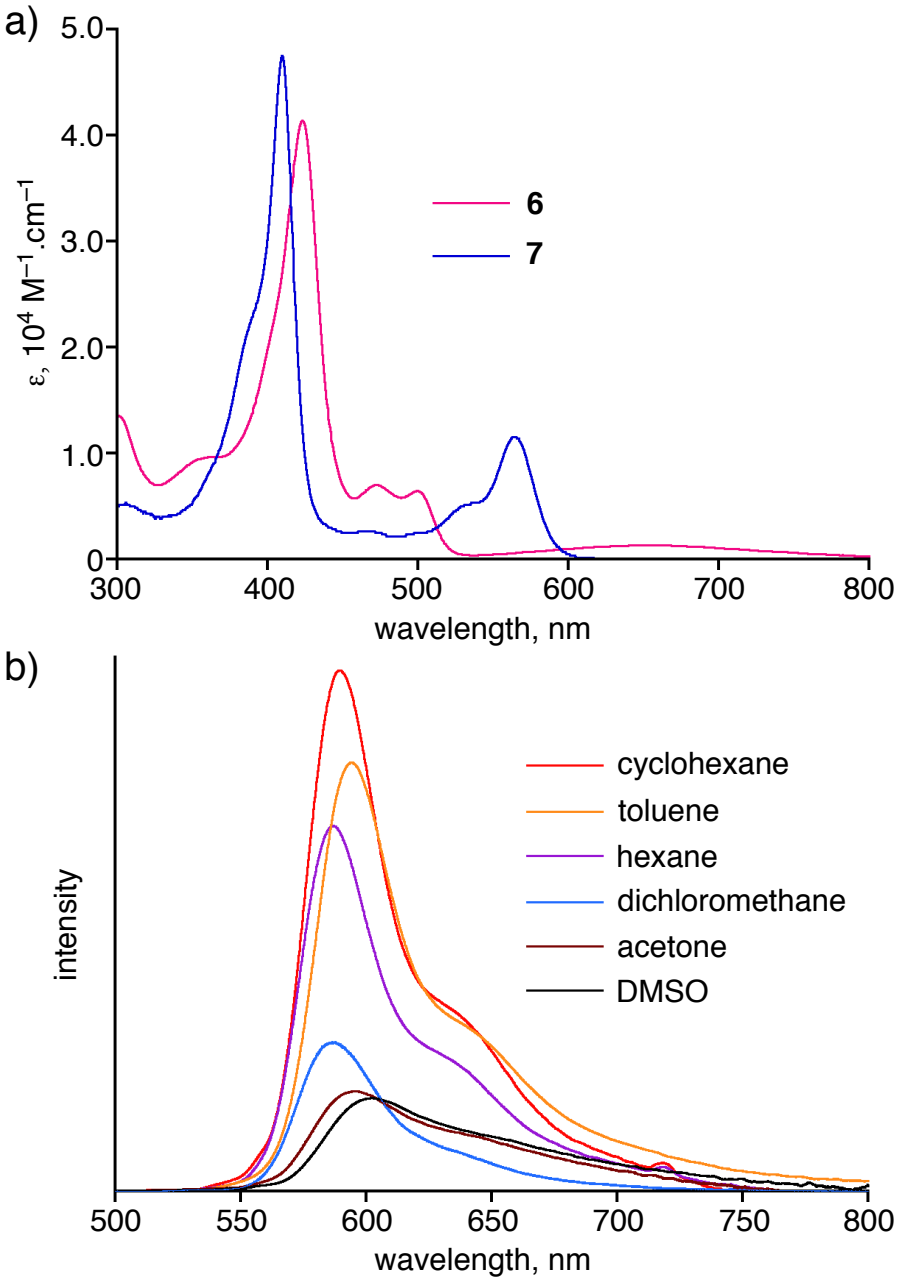

Fig 4. (a) Top and (b) side views of X-ray crystal structure of **6**. Mesityl and 4-methoxybenzyl groups as well as hydrogen atoms are omitted for clarity. Thermal ellipsoids are at the 50% probability level.

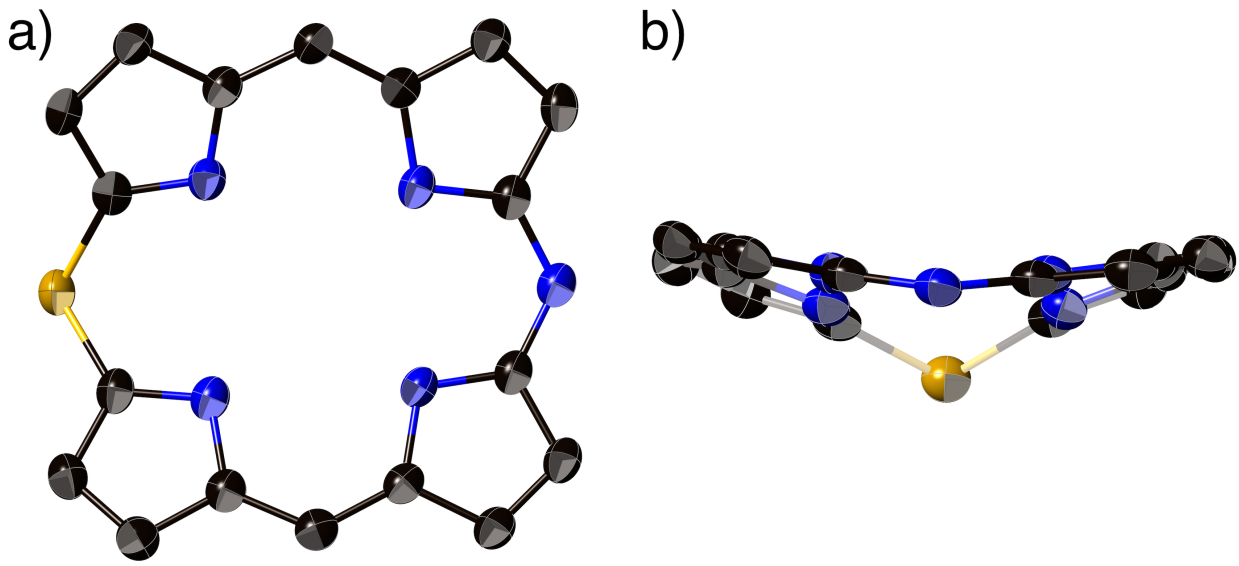

Fig 5. (a) NICS values of **6** calculated at the GIAO-B3LYP/def2-TZVP level. (b) ACID plot of **6** (isovalue 0.03) calculated at the CSGT-B3LYP/def2-TZVP level.

a)

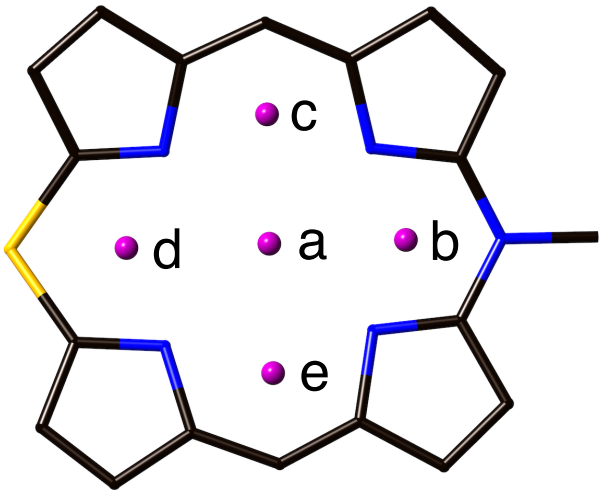

position	NICS
a	11.4
b	12.9
c	14.3
d	11.7
e	14.1

b)